to GCC

(5) p. 7

529115

Troposphere-stratosphere dynamic coupling under strong and weak polar vortex conditions

Judith Perlwitz[1]
NASA Goddard Institute for Space Studies, New York, USA

Hans-F. Graf
Max Planck Institute for Meteorology, Hamburg, Germany

Abstract

The relationship between Northern Hemisphere (NH) tropospheric and stratospheric wave-like anomalies of spherical zonal wave number (ZWN) 1 is studied by applying Canonical Correlation Analysis (CCA). A lag-correlation technique is used with 10-day lowpass filtered daily time series of 50- and 500-hPa geopotential heights. Generally stratospheric circulation is determined by ultralong tropospheric planetary waves. During winter seasons characterized either by an anomalously strong or weak polar winter vortex different propagation characteristics for waves of ZWN 1 are observed. The non-linear perspective of the results have implications for medium range weather forecast and climate sensitivity experiments.

Introduction

A principal concept for the description of the mutual dynamic coupling between troposphere and stratosphere (T-S coupling) is based on wave-mean flow interaction [*Charney and Drazin,* 1961; *Matsuno,* 1970]. Ultra-long planetary waves, generated by orography and diabatic heating, propagate into the middle atmosphere and modify the mean flow by transferring heat and momentum. The strength of the stratospheric polar vortex determines the transmission-refraction properties of these vertically propagating waves, and, thus, modifies the structure of ultra-long tropospheric waves. Finding evidence in observations for this coupling is necessary to verify this theoretical concept. The characteristic features of the coupling are also very important in validating the capability of atmospheric general circulation models (GCMs) to reproduce this dynamic process.

On the basis of observational data, *Randel* [1988] studied the propagation characteristics in the vertical direction on a two-dimensional plane for individual waves of ZWN 1 to 3 at 51°N. Both observational data and experiments with atmospheric GCMs show a downward propagation of zonal mean zonal wind anomalies from the mesosphere into the upper troposphere resulting from the interaction of vertically propagating waves with the mean flow [*Kodera et al.,* 1996; *Kuroda and Kodera,* 1999; *Baldwin and Dunkerton,* 1999]. The changes in the mean flow are strongly related to a change in the meridional propagation of tropospheric waves. Composites of the refraction index and the Eliassen-Palm Flux indicate that the southward propagation of tropospheric waves is strongly increased in winter months with an anomalously strong stratospheric polar winter vortex [*Kodera et al.,* 1996; *Limpasuvan and Hartmann,* 2000; *Kuroda and Kodera,* 1999].

In the present paper, a statistical-dynamic approach is applied to isolate hemispheric scale characteristic features of the vertical propagation of ultra-long spherical wave-like anomalies in the NH using observational data. The differences in these features in winter seasons characterized either by an anomalously strong or weak polar winter vortex are discussed. Using 90-day low-pass filtered daily data, *Baldwin and Dunkerton* [1999] showed that the Arctic Oscillation, which is a more zonally symmetric pattern, takes about three weeks to propagate from the 10-hPa level to the surface due to wave-mean flow interaction. We applied a process-oriented spatial filtering and only a small temporal filtering to study relevant processes of dynamic T-S coupling in more detail.

Statistical-Dynamic Approach and Data

Our statistical-dynamic approach single wave analysis (SWAN) combines the well-known theoretical concept of dynamic T-S coupling by *Charney and Drazin* [1961] with the statistical data analysis. The main implication of the Charney-Drazin Theorem for our understanding of the dynamical coupling between troposphere and stratosphere is as follows: Vertically propagating waves are selectively reflected at levels of supercritical westerly zonal velocity. This critical Rossby velocity decreases with increasing ZWN and depends on the latitude. SWAN is physically based on this theorem. Multivariate SWAN comprises the investigation of the relationship between a tropospheric and a stratospheric spherical wave field of geopotential heights with multivariate statistical analysis methods. The geopotential heights fields were decomposed in Fourier harmonics and the Fourier coefficients were used to recompose the temporal height field for single zonal waves. Unlike *Randel* [1988], we study vertical wave propagation for the whole NH extratropics instead selecting one specific latitude.

To study the linear statistical relationship between a tropospheric (500-hPa) and a stratospheric (50-hPa) geopotential height field for a single zonal wave, CCA according to *Barnett and Preisendorfer* [1987] was used. By applying CCA with lag-correlations on the daily time series, the time lag at which both wave fields are maximally correlated can be determined. The canonical correlation coefficient $r_{CCA}(lag)$ is the unambiguous measure of the maximum correlation indicating the time lag of maximally related anomaly patterns of the 500- and 50-hPa wave fields.

For the physical interpretation of the CCA results, we also take into account that the propagation of wave energy in vertical and meridional direction is accompanied by a longitudinal phase shift. The tilt in vertical and meridional direction of planetary waves of a specific ZWN can be used to recognize this physical process in associated anomaly patterns isolated, for example, by CCA. The up- and downward propagation of wave anomalies is related to a west- and eastward tilt of waves with increasing height, respectively [e.g., *James,* 1994, page 195]. A west- and eastward tilt of the waves with increasing latitude characterizes pole- and equatorward propagation, respectively [e.g., *Kodera and Chiba*, 1995].

The daily 50- and 500-hPa geopotential heights used for this study were based on the National Centers for Environmental Prediction-National Center for Atmospheric Research (NCEP-NCAR) reanalysis [*Kalnay et al.*, 1996]. The data of the time period from 1958 to 1999 were statistically analyzed on a $5° \times 5°$ grid, north of 30°N. The lowpass filtered daily data (December to February) were determined on the basis of the 21-point filter by *Blackmon and Lau* [1980] by which synoptic scale disturbances (< 10 days) were removed. This filtering does not influence the results significantly. Using unfiltered daily data, we found slightly reduced canonical correlation coefficients due to the higher variability. The mean seasonal cycles were removed and the grid-point time series were weighted with the square root of the cosine of the latitude prior to the analyses to give all grid points equal area-weight. According to the CCA approach by *Barnett and Preisendorfer* [1987] the datasets were pre-filtered by retaining only the projection of each field on a subset of its empirical orthogonal functions (EOFs) before applying CCA. We used the first two EOFs of the stratospheric fields and the first four EOFs of the tropospheric field which explain about 90% of the total variance of the ZWN 1 wave fields. Two coupled modes can be isolated. As defined in the CCA, the temporal expansion coefficients of the second coupled mode are ambiguously determined by the first mode. Thus, only the first coupled mode will be interpreted.

Results

The approach described above is used to isolate the characteristic hemispheric scale features of the vertical propagation of tropospherically forced waves for winter seasons (December to February) characterized either by an anomalously weak or strong polar winter vortex. An index for the strength of the stratospheric polar winter vortex was defined by the temporal expansion coefficient of the first EOF of the NH 50-hPa geopotential height winter means. This EOF is a very good indication of the variation in the strength of the polar winter vortex [*Kodera et al.*, 1996]. The standardized expansion coefficients of the first EOF are shown in Figure 1. We call winter seasons characterized by an anomalously strong (positive index $> 0.5\,\sigma$) and by an anomalously weak (negative index $< -0.5\,\sigma$) polar winter vortex S-PVS (strong polar-vortex-season) and W-PVS (weak polar-vortex-season), respectively. We composed the 10-day lowpass filtered daily time series of the NH 50- and 500-hPa geopotential heights of the winter months into one S-PVS (15 seasons) and one W-PVS (13 seasons) ensemble. For each ensemble, we carried out a series of CCAs by varying the time lag $(-10, -9, \ldots, 0, \ldots, 9, 10)$ between the time series of the 50- and 500-hPa ZWN 1 fields. Taking the stratospheric field as reference level, a time lag of -10 (10) indicates that the tropospheric (stratospheric) time series leads the stratospheric (tropospheric) by 10 days.

The correlation coefficients of the first mode of the two CCA series are shown in Figure 2. The graph of $r_{CCA}(lag)$ of the first coupled mode for the W-PVS analysis series exhibits a pronounced increase from 0.50 at lag 0 to 0.64 at a time lag of -4 to -5 days. With increasing positive time lag a strong drop of $r_{CCA}(lag)$ to 0.25 at a time lag of 10 days is found. This course indicates the expected influence of mid-tropospheric waves on the structure of waves in the lower stratosphere. In Figure 3, the homogeneous regression pattern of the 500-hPa ZWN 1 field and the heterogeneous regression pattern of the 50-hPa ZWN 1 field are shown for the '-4 days-lag CCA', i.e. the time series of both ZWN 1 fields were regressed onto the standardized temporal expansion coefficients of the 500-hPa canonical pattern. Thus, the regression coefficients represent the typical amplitude in [gpm] corresponding to the anomalies of one standard deviation of the index time series. The shading indicates where the respective correlation coefficients are significant at least at the 99% confidence level. The largest amplitudes of the wave field at the 500-hPa level appear between 50° and 70°N, and the maxima are located over the North Atlantic and Eastern Asia. At about the same longitude, wave anomalies with opposite sign are present at low latitudes. The maxima of the related 50-hPa ZWN 1 pattern four days later are shifted westward relative to the maxima at the 500-hPa level by about 80°. Thus, the process which is described by the first mode of the '-4 days-lag CCA' is the upward propagation of tropospherically forced waves of ZWN 1 into the stratosphere. The propagation time from the 500- to the 50-hPa level amounts to 4 - 5 days. This vertical propagation is most relevant between 50° and 70°N.

The $r_{CCA}(lag)$ of the first coupled mode for the S-PVS clearly show a different course than the $r_{CCA}(lag)$ for the W-PVS (Figure 2). Two maxima are found, one at a negative time lag of −2 to −3 days and a second one at a positive lag of 6 days. The maximum at negative time lags in the S-PVS appears earlier and is somewhat smaller than the maximum in the W-PVS. This result corresponds to the derivation of the vertical group velocity of Rossby waves [*Andrews et al.*, 1987] indicating that, for stationary waves, the group velocities increase with increasing zonal mean zonal wind. Figure 4 shows the associated patterns for the '−2 days-lag CCA' in the S-PVS. A smaller westward tilt of the waves with increasing height appears in the associated patterns during S-PVS (about 50°) than during W-PVS (about 80°) which corresponds to the faster vertical propagation during S-PVS. The heterogeneous regression patterns of the 50-hPa geopotential heights of both ensembles also reveal that during S-PVS, an equatorward propagation occurs (eastward tilt with increasing latitude), which is not obvious during W-PVS.

The most obvious difference in the course of $r_{CCA}(lag)$ of the first coupled modes between the S-PVS and W-PVS ensembles (Figure 2) is the second maximum at a positive time lag of 6 days for the S-PVS. This result reveals that only during S-PVS a strong downward influence occurs which is not relevant during W-PVS. Figure 5 shows the associated regression patterns when the time series of the stratospheric field leads that of the tropospheric field by 6 days. For this figure, we regressed the wave fields of both pressure levels to the standardized temporal expansion coefficients of the stratospheric canonical pattern. The 500-hPa pattern very clearly exhibits an eastward tilt of the waves of the ZWN 1 with increasing latitude. In addition, the associated patterns in Figure 5 show an eastward phase shift with increasing height at higher latitudes. Thus, the process which is described by the first mode of the '6 days-lag CCA' is downward refraction at around 65°N from the stratosphere to the mid-troposphere and a southward propagation of wave energy of ZWN 1 in the mid-troposphere.

Discussion and Conclusions

We compared the vertical propagation characteristics of NH spherical waves of ZWN 1 in winter seasons characterized either by an anomalously strong or weak polar winter vortex by applying a multivariate SWAN. The study of all winter season (not shown) and especially of winter seasons characterized by an anomalously weak stratospheric polar winter vortex (W-PVS) illustrates that the upward propagation of wave-like anomalies from the troposphere into the stratosphere is the dominating feature of the dynamical coupling between both atmospheric layers. However, during winter seasons with an anomalously strong polar winter vortex (S-PVS) the structure of waves of ZWN 1 in the mid-troposphere is changed on a hemispheric scale due to the downward and southward refraction of wave energy of ZWN 1. This result supports our understanding about the influence of the distribution of the zonal mean zonal wind distribution on the transmission-refraction properties of vertically propagating ultralong waves. The regions of critical Rossby velocities are a bifurcation for the vertical propagation of these waves up to higher altitudes. Such influence can be expected also for waves of ZWN 2 and 3 which have different critical Rossby velocities and faster vertical propagation times than waves of ZWN 1 [*Randel*, 1988].

In the wintertime, the Arctic polar stratospheric vortex can be distorted due to nonlinear breaking of vertically propagating waves from the troposphere and by eastward traveling waves within the stratosphere. On the basis of a case study, *Hartley et al.* [1998] showed that this process of stratospheric vortex distortions has a simultaneous feedback to the circulation at the tropopause. Near 60°N, the induced geopotential height pattern at the tropopause has a similar ZWN 1 structure as shown in Figure 5a.

The difference in the propagation characteristics for waves of ZWN 1 during the W-PVS and S-PVS has numerous implications. Firstly, low frequency variability (interannual) has a direct influence on high frequency (intraseasonal) variability structure. The exaggeration of an anomalously strong polar winter vortex by external forcing [for a review, *Shindell et al.*, 2000] or internal variability [*Perlwitz et al.*, 2000] may lead to nonlinear changes in the tropospheric circulation.

Secondly, given that many current climate models are biased towards a too strong polar winter vortex, they may only reflect the S-PVS regime and, hence, may underestimate any nonlinear climate changes due to the neglect of the bifurcation of T-S coupling at the critical Rossby velocity. A realistic representation of the stratospheric mean state and the processes of the dynamic troposphere-stratosphere coupling are also highly important for medium-range weather forecast models.

Finally, observational results like the ones presented in this study can be used to evaluate atmospheric GCMs in a process-oriented way.

Acknowledgments. We would like to thank David Rind, Gavin Schmidt, Nambath K. Balachandran and the two unknown reviewer for helpful comments on the manuscript.

References

Andrews, D. G., J. Holton, and C. B. Leovy, *Middle Atmosphere Dynamics*, Academic Press, pp 489, 1987.

Baldwin, M. P., and T. J. Dunkerton, Propagation of the Arctic Oscillation from the stratosphere to the troposphere, *J. Geophys. Res., 104*, 30937-30946, 1999.

Barnett, T. P., and R. Preisendorfer, Origins and levels of monthly and seasonal forecast skill for United States surface air temperatures determined by canonical correlation analysis, *Mon. Wea. Rev.*, *115*, 1825-1850, 1987.

Blackmon, M. L., and N. C. Lau, Regional characteristics of the Northern Hemisphere wintertime circulation: a comparison of the simulation of a GFDL general circulation model with observations, *J. Atmos. Sci.*, *37*, 497–514, 1980.

Charney, J. G., and P. G. Drazin, Propagation of planetary-scale disturbances from the lower into the upper atmosphere, *J. Geophys. Res., 66*, 83-109, 1961.

Hartley, D. E., J. T. Villarin, R. X. Black and C. A. Davis, A new perspective on the dynamical link between the stratosphere and troposphere, *Nature, 391*, 471-474, 1998.

Kalnay, E., et al., The NCEP/NCAR 40-year reanalysis project, *B. Am. Meteorol. Soc.*, *77*, 437-471, 1996.

Kodera, K., and M. Chiba, Tropospheric circulation changes associated with stratospheric sudden warmings: A case study, *J. Geophys. Res., 100*, 11055-11068, 1995.

Kodera, K., M. Chiba, H. Koide, A. Kitoh, and Y. Nikaidou, Interannual variability of the winter stratosphere and troposphere, *J. Meteor. Soc. Japan, 74*, 365-382, 1996.

Kuroda, K., and K. Kodera, Role of planetary waves in the stratosphere-troposphere coupled variability in the northern hemisphere winter, *Geophys. Res. Lett., 26*, 2375-2378, 1999.

Limpasuvan, V., and D. L. Hartmann, Wave-maintained annular modes of climate variability, *J. Clim., in press*, 2000.

Matsuno, T., Vertical propagation of stationary planetary waves in the winter Northern Hemisphere, *J. Atmos. Sci., 27*, 871-883, 1970.

Perlwitz, J., H.-F. Graf, and R. Voss, The leading mode of the coupled troposphere-stratosphere winter circulation in different climate regimes, *J. Geophys. Res.*, *105*, 6915-6926, 2000.

Randel, W. J., Further modification of time-longitude lag-correlation diagrams: Application to three-dimensional wave propagation, *Tellus*, *40A*, 257–271, 1988.

Shindell, D. T., G. A. Schmidt, R. L. Miller, and D. Rind, Northern Hemisphere winter climate response to greenhouse gas, ozone, solar and volcanic forcing, *J. Geophys. Res.*, in press, 2000.

J. Perlwitz, NASA-GISS, 2880 Broadway, New York, NY, 10025, USA. (e-mail: judith@giss.nasa.gov)

H.-F. Graf, Max Planck Institute for Meteorology, Bundesstrasse 55, D-20146 Hamburg, Germany. (e-mail: graf@dkrz.de)

[1]Also at Center for Climate Systems Research, Columbia University, New York.

This preprint was prepared with AGU's LaTeX macros v5.01. File tswavcont2 formatted November 1, 2000.

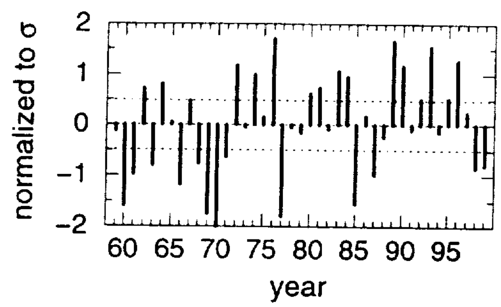

Figure 1. Expansion coefficients of the first EOF of the NH (north of 30°N) geopotential heights, determined on the basis of winter means. The time series is normalized to the standard deviation (σ).

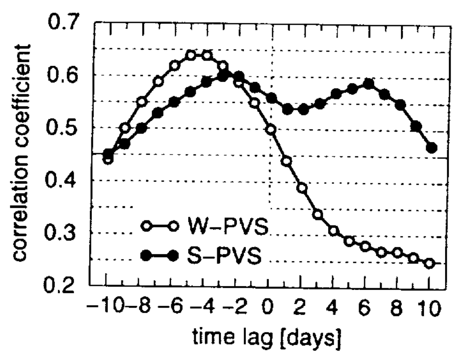

Figure 2. Canonical correlation coefficients of CCA series of different time lags for the 50- and 500-hPa height fields, recomposed by waves of ZWN 1 for both the W-PVS and S-PVS ensembles. A positive time lag indicates that the time series of the stratospheric field leads the time series of the tropospheric field and vice versa.

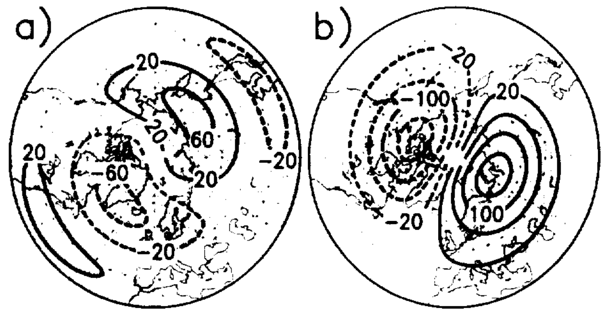

Figure 3. Maps of (a) homogeneous regression coefficients [gpm] of the 500-hPa ZWN 1 field and (b) heterogeneous regression coefficients [gpm] of the 50-hPa ZWN 1 field for the '−4 days-lag CCA' in the W-PVS ensemble. The shading indicates where the homogeneous (a) and heterogeneous (b) correlation coefficients are significant at least at the 99% confidence level.

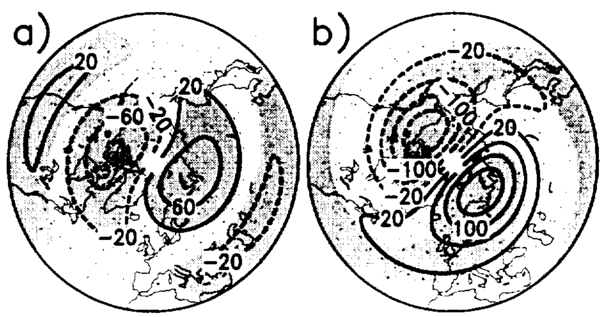

Figure 4. Same as Figure 3 but for '−2 days-lag CCA' in the S-PVS ensemble.

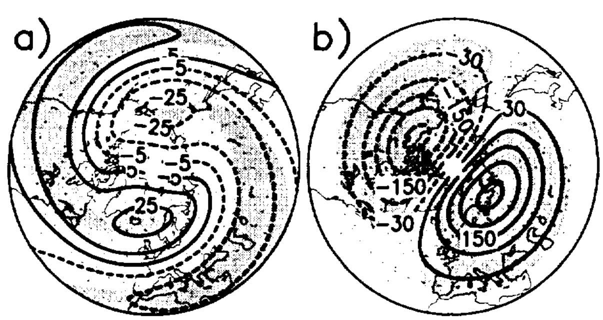

Figure 5. Maps of (a) heterogeneous regression coefficients [gpm] of the 500-hPa ZWN 1 field and (b) homogeneous regression coefficients [gpm] of the 50-hPa ZWN 1 field for the '6 days-lag CCA' in the S-PVS ensemble. The shading corresponds to Figure 3.